Inorg. Chem. **2006**, *45*, 9758–9764

SHG Active Crystals of a Remote Functionalized Achiral NLO-phore Assembled through Zinc(II) Complexation

M. Jaya Prakash and T. P. Radhakrishnan*

School of Chemistry, University of Hyderabad, Hyderabad-500 046, India

Received June 23, 2006

An achiral nonlinear optical chromophore with a "remote functionality" that can act as a ligand is developed on the basis of 4-nitroaniline derivatized with pyridine. The molecules are assembled through complexation with simple achiral zinc(II) salts and the H-bond network mediated by the counterions, to generate noncentrosymmetric materials exhibiting optical second harmonic generation (SHG). The crystal structures of the new complexes are determined; the counterion strongly influences the ligand orientations and lattice structure. SHG of the microcrystalline materials is investigated. Correlation between the structure and SHG is rationalized using semiempirical quantum chemical estimation of the hyperpolarizabilities of molecules and molecular clusters. The metal complexation plays a significant role in molecular assembly but affects the SHG very little, enabling simplified analysis of the bulk property in terms of molecular responses. Organization of remote functionalized molecules by metal ion complexation thus offers a convenient approach to the rational design of quadratic NLO materials.

Introduction

Development of novel molecular materials for quadratic nonlinear optical (NLO) applications such as second harmonic generation (SHG) is realized through two major steps. The first is the synthesis of the molecular unit, preferably with a large hyperpolarizability (β), and the second involves the assembly of these molecular building blocks with optimal orientation of the β tensor components that maximizes the NLO response of the bulk material. From the applications perspective, it is highly desirable that the materials have a wide transparency window in the wavelength range of interest and good thermal and chemical stability. While the first level of molecule (NLO-phore) synthesis has been widely explored both theoretically and experimentally,[1] the more complex problem of assembly involves fundamental questions of intermolecular interactions and molecular organization in crystals and thin films. The even order nature of the NLO effect of SHG necessitates a noncentrosymmetric structure for the material; optimal orientation of the molecules can lead to enhanced responses.[2] Several chemical[3] and physical[4] approaches have been implemented to fabricate molecular materials exhibiting SHG response. Organization of a specific NLO-phore unit into different lattice structures and examination of their SHG responses would provide useful insight into the efficacy of the various assembly

* To whom correspondence should be addressed. E-mail: tprsc@uohyd.ernet.in. Phone: 91-40-2301-1068. Fax: 91-40-2301-2460.

(1) (a) Zyss, J.; Ledoux, I. *Chem. Rev.* **1994**, *94*, 77. (b) Kanis, D. R.; Ratner, M. A.; Marks, T. J. *Chem. Rev.* **1994**, *94*, 195. (c) Marks, T. J.; Ratner, M. A. *Angew. Chem., Int. Ed. Engl.* **1995**, *34*, 155.

(2) (a) Chemla, D. S., Zyss, J., Eds. *Nonlinear Optical Properties of Organic Molecules and Crystals*; Academic Press: New York, 1987; Vol. 1. (b) Nie, W. *Adv. Mater.* **1993**, *5*, 520. (c) Zyss, J.; Nicoud, J. F. *Curr. Opin. Solid State Mater. Sci.* **1996**, *1*, 533.

(3) (a) Rieckhoff, K.; Peticolas, W. F. *Science* **1965**, *147*, 610. (b) Levine, B. F.; Bethea, C. G.; Thurmond, C. D.; Lynch, R. T.; Bernstein, J. L. *J. Appl. Phys.* **1979**, *50*, 2523. (c) Lipscomb, G. F.; Garito, A. F.; Narang, R. S. *J. Chem. Phys.* **1981**, *75*, 1509. (d) Eaton, D. F. *Science* **1991**, *253* , 281. (e) Zyss, J. *J. Phys. D* **1993**, *26*, B198. (f) Dalton, L. R.; Harper, A. W.; Robinson, B. H. *Proc. Natl. Acad. Sci. U.S.A.* **1997**, *94*, 4842. (g) Gangopadhyay, P.; Sharma, S.; Rao, A. J.; Rao, D. N.; Cohen, S.; Agranat, I.; Radhakrishnan, T. P. *Chem. Mater.* **1999**, *11*, 466. (h) Gangopadhyay, P.; Rao, S. V.; Rao, D. N.; Radhakrishnan, T. P. *J. Mater. Chem.* **1999**, *9*, 1699. (i) Gangopadhyay, P.; Radhakrishnan, T. P. *Chem. Mater.* **2000**, *12*, 3362. (j) Gangopadhyay, P.; Srinivas, N. K. M. N.; Rao, D. N.; Radhakrishnan, T. P. *Opt. Mater.* **2002**, *21*, 55.

(4) (a) Weissbuch, I.; Lahav, M.; Leiserowitz, L.; Meredith, G. R.; Vanherzeele, H. *Chem. Mater.* **1989**, *1*, 114. (b) Serbutovicz, C.; Nicoud, J. F.; Fischer, J.; Ledoux, I.; Zyss, J. *Chem. Mater.* **1994**, *6*, 1358. (c) Ramamurthy, V.; Eaton, D. F. *Chem. Mater.* **1994**, *6*, 1128. (d) Burland, D. M.; Miller, R. D.; Walsh, C. A. *Chem. Rev.* **1994**, *94*, 31. (e) Ashwell, G. J.; Jackson, D. P.; Crossland, W. A. *Nature (London)* **1994**, *368*, 438. (f) Hoss, R.; Konig, O.; Kramer-Hoss, V.; Berger, U.; Rogin, P.; Hulliger, J. *Angew. Chem., Int. Ed. Engl.* **1996**, *35*, 1664. (g) Ulman, A. *Chem. Rev.* **1996**, *96*, 1533. (h) Miyata, S., Sasabe, H., Eds. *Poled Polymers and their Applications to SHG and EO Devices*; Gorden and Breach Science Publishers: Amsterdam, 1997. (i) Forrest, S. R. *Chem. Rev.* **1997**, *97*, 1793. (j) Lvov, Y.; Ariga, K.; Onda, M.; Ichinose, I.; Kunitake, T. *Colloids Surf., A* **1999**, *146*, 337. (k) Park, S. Y.; Rubner, M. F.; Mayes, A. M. *Langmuir* **2002**, *18*, 9600. (l) Cui, X.; Pei, R.; Wang, Z.; Yang, F.; Ma, Y.; Dong, S.; Yang, X. *Biosens. Bioelectron.* **2003**, *18*, 59.

10.1021/ic061145v CCC: $33.50
Published on Web 11/02/2006

Table 1. Crystallographic Data for PINA-C, PINA-N, ZPA, and ZPP

param	PINA-C	PINA-N	ZPA	ZPP
empirical formula	$C_{12}H_{11}N_3O_2$	$C_{12}H_{11}N_3O_2$	$C_{28}H_{28}N_6O_8Zn$	$C_{30}H_{32}N_6O_8Zn$
cryst system	orthorhombic	monoclinic	monoclinic	orthorhombic
space group	Pbca	Pn	Pn	$C222_1$
a/Å	11.3657(8)	4.5747(18)	10.406(4)	13.6852(9)
b/Å	7.7206(6)	10.194(4)	10.387(4)	16.1279(11)
c/Å	24.7787(18)	12.037(5)	14.203(6)	13.7491(9)
β/deg	90.0	99.730(6)	108.928(6)	90.0
V/Å^3	2174.3(3)	553.3(4)	1452.2(10)	3034.6(3)
Z	8	2	2	4
ρ_{calc}/g cm^{-3}	1.401	1.376	1.468	1.466
μ/mm^{-1}	0.099	0.097	0.906	0.870
temp/K	298(2)	298(2)	298(2)	298(2)
λ/Å	0.710 73	0.710 73	0.710 73	0.710 73
min, max transm	0.8917, 0.9853	0.6829, 0.9923	0.5677, 0.8991	0.7208, 0.9028
Flack param		a	0.053(8)	0.011(13)
no. of reflcns	2631	2546	6574	3641
no. of params	154	154	390	205
GOF	1.082	1.172	0.933	1.085
R (for $I \geq 2\sigma_I$)	0.0586	0.0692	0.0486	0.0407
wR^2	0.1394	0.1598	0.0649	0.0915
largest diff peak, hole/e Å^{-3}	0.206, −0.326	0.219, −0.220	0.555, −0.293	0.585, −0.200

[a] Not refined.

motifs. In this context, we have considered a general approach on the basis of what can be termed as "remote-functionalized NLO-phores". Since the assembly of these units is primarily mediated by the remote-functional group that is not in conjugation with the π-electron system of the NLO-phore, the variations in the SHG response of the bulk materials will be dominated by the assembly patterns with the molecular response remaining largely invariant.

We have investigated several organic molecular materials based on remote functionalized chromophores and NLO-phores. The interesting phenomena demonstrated include charge transfer occurring exclusively in the solid state,[5] enhanced fluorescence in the solid state and doped polymer films,[6] and the realization of noncentrosymmetric crystal lattices and second harmonic generation from achiral[7] as well as chiral molecular units.[8] In this study, we have explored a new avenue on the basis of metal complexation for the assembly of remote functionalized NLO-phores to fabricate SHG active materials. Metal complexation is a convenient approach to assemble molecular NLO materials; however, the metal ions bound to the chromophore units affect their electronic structure and hence NLO response, making any analysis of the SHG from the bulk material and further design/development complicated. In many instances, the metal ion complexation may have the detrimental effect of reducing the hyperpolarizability of the molecular NLO-phores and thus the SHG response of the material. The remote functional approach outlined above is expected to circumvent these difficulties. We have chosen the classical NLO-phore on the basis of the push−pull system, 4-nitroaniline (pNA), and introduced 4-picolyl group as the remote functionality to aid in the assembly through metal complexation; the resulting molecule is *N*-(4-picolyl)-4-nitroaniline, PINA. Zinc(II) was chosen as the metal ion since it affords materials with good transparency window as well as thermal stability.[9,10] This paper presents, first, the polymorphic structures of centrosymmetric as well as noncentrosymmetric crystals formed by the ligand, PINA, designated respectively as PINA-C and PINA-N. Investigation of complexes of PINA with a variety of achiral Zn(II) salts showed that several (acetate, propionate, succinate, maleate) form SHG active materials. The crystals of the complexes derived from the acetate and propionate salts of Zn(II), $Zn(PINA)_2X_2$ (X = acetate, ZPA, and X = propionate, ZPP) were amenable to structure analysis and are presented here. SHG measurements on the microcrystalline powders of PINA as well as the Zn-(II) complexes are reported. The trends are examined using quantum chemical estimations of the hyperpolarizability of molecules and molecular clusters and qualitative considerations of the NLO-phore orientations that are influenced by the extended H-bonded network formations in the two crystals. The study illustrates the utility of metal complexation of remote functionalized molecules as a convenient and rational approach to the assembly of novel molecular SHG materials.

Experimental Section

Synthesis and Characterization. *N*-(4-Picolyl)-4-nitroaniline (PINA). A 2.0 g amount of K_2CO_3 was added to 30 mL of DMSO, and the solution was stirred for 15 min. A 0.713 g (0.67 mL, 6.6 mmol) amount of 4-picolylamine and 0.913 g (0.68 mL, 6.6 mmol) of 4-fluoronitrobenzene were added, and the reaction mixture was

(5) Jayanty, S.; Radhakrishnan, T. P. *Chem. Mater.* **2001**, *13*, 2072.
(6) Jayanty, S.; Radhakrishnan, T. P. *Chem.—Eur. J.* **2004**, *10*, 791.
(7) (a) Jayanty, S.; Gangopadhyay, P.; Radhakrishnan, T. P. *J. Mater. Chem.* **2002**, *12*, 2792. (b) Jayanty, S.; Radhakrishnan, T. P. *Chem.—Eur. J.* **2004**, *10*, 2661. (c) Prakash, M. J.; Radhakrishnan, T. P. *Chem. Mater.* **2006**, *18*, 2943.
(8) Prakash, M. J.; Radhakrishnan, T. P. *Cryst. Growth Des.* **2005**, *5*, 1831.
(9) (a) Qin, J.; Liu, D.; Dai, C.; Chen, C.; Wu, B.; Yang, C.; Zhan, C. *Coord. Chem. Rev.* **1999**, *188*, 23. (b) Xiong, R.; Zuo, J.; You, X.; Fun, H.; Raj, S. S. S. *New J. Chem.* **1999**, *23*, 1051. (c) Xiong, R.; Zuo, J.; You, X.; Abrahams, B. F.; Bai, Z.; Che, C.; Fun, H. *Chem. Commun.* **2000**, 2061. (d) Tian, Y.; Yu, W.; Zhao, C.; Jiang, M.; Cai, Z.; Fun, H. *Polyhedron* **2002**, *21*, 1217. (e) Chen, Y.; Zhang, J.; Cheng, J.; Kang, Y.; Li, Z.; Yao, Y. *Inorg. Chem. Commun.* **2004**, *7*, 1139. (f) Kim, Y.; Martin, S. W.; Ok, K. M.; Halasyamani. P. S. *Chem. Mater.* **2005**, *17*, 2046.
(10) Evans, C.; Luneau, D. *J. Chem. Soc., Dalton Trans.* **2002**, 83.

stirred for 12 h at 30 °C. Ice mixed with water was added and stirred for 15 min. The yellow precipitate formed was filtered out, washed with cold water, and dried under vacuum; yield = 49.6%. The crude product was recrystallized by diffusing hexane vapors into a solution in ethyl acetate yielding crystals of PINA-C: mp/°C = 145−147; FT-IR (KBr) $\bar{\nu}$/cm^{-1} = 3231.0, 3013.1, 1603.0, 1570.0, 1510.0, 1475.7, 1113.0; ^{1}H NMR (DMSO-d_6) δ/ppm = 4.47 (d, 2H), 6.64 (d, 2H), 7.30 (d, 2H), 7.86 (t, 1H), 7.96 (d, 2H), 8.50 (d, 2H); ^{13}C NMR (DMSO-d_6) δ/ppm = 45.21, 111.70, 122.61, 126.61, 136.83, 148.33, 150.17, 154.63. Needle-shaped crystals of PINA-N were grown from a mixture of acetonitrile and water (6:4 v/v).

Zn(PINA)$_2$(CH$_3$COO)$_2$ (ZPA). A solution of 0.025 g (0.11 mmol) of PINA in 2 mL of methanol was mixed with a solution of 0.024 g (0.11 mmol) of zinc acetate in 2 mL of methanol and kept at 30 °C. Crystals of the complex formed in 3 days were filtered out, washed, and dried: yield = 84.5%; mp/°C = 162−164; FT-IR (KBr): $\bar{\nu}$/cm^{-1} = 3312.1, 3134.6, 3069.0, 1603.0, 1560.3, 1504.6, 1477.6, 1111.1; ^{1}H NMR (DMSO-d_6) δ/ppm = 1.80 (s, 6H), 4.50 (d, 4H), 6.63 (d, 4H), 7.39 (d, 4H), 7.87(t, 2H), 7.96 (d, 4H), 8.52-(d, 4H); ^{13}C NMR (DMSO-d_6) δ/ppm = 22.89, 45.15, 111.75, 123.01, 126.62, 136.90, 149.70, 149.90, 154.56, 171.43.

Zn(PINA)$_2$(C$_2$H$_5$COO)$_2$ (ZPP). A solution of 0.025 g (0.11 mmol) of PINA in 2 mL of methanol was mixed with a solution of 0.025 g (0.11 mmol) of zinc propionate in 3 mL of methanol and kept at 30 °C. Crystals of the complex formed in 4 days were filtered out, washed, and dried: yield = 80.6%; mp/°C = 136−138; FT-IR (KBr): $\bar{\nu}$/cm^{-1} = 3315.9, 3120.0, 3069.0, 2949.4, 1610.0, 1595.3, 1506.5, 1483.4, 1109.2; ^{1}H NMR (DMSO-d_6) δ/ppm = 0.95 (t, 6H), 2.10 (m, 4H), 4.52 (d, 4H), 6.64 (d, 4H), 7.42 (d, 4H), 7.89 (m, 2H), 7.96 (d, 4H), 8.53 (d, 4H); ^{13}C NMR (DMSO-d_6) δ/ppm = 10.98, 28.91, 45.15, 111.76, 123.16, 126.70, 136.94, 149.79, 150.49, 154.52, 180.46.

Crystallography. X-ray diffraction data were collected on a Bruker Nonius Smart Apex diffractometer (with CCD detector). Mo Kα radiation with a graphite crystal monochromator in the incident beam was used. Data were reduced using SAINT; all non-hydrogen atoms were found using the direct method analysis in SHELXTL, and after several cycles of refinement, positions of the hydrogen atoms were calculated and added to the refinement process.[11] The Flack parameter was refined for the zinc complexes. Details of data collection, solution, and refinement, as well as the crystallographic information files, are submitted as Supporting Information.

SHG Measurement. Second harmonic generation from microcrystalline powders was examined using the Kurtz−Perry[12] method. Identity of the powder samples was ensured and presence of polymorphic structures ruled out by verifying the agreement between experimental powder X-ray patterns and those simulated from the single-crystal structure (see Supporting Information). Particle sizes were graded using standard sieves; sizes ranging from 40 to 300 μm were studied. Samples were loaded in glass capillaries having an inner diameter of 600 μm. The fundamental beam (1064 nm) of a Q-switched ns-pulsed (6 ns, 10 Hz) Nd:YAG laser (Spectra Physics model INDI-40) was used. The second harmonic signal was collected using appropriate optics and detected using a monochromator, PMT, and oscilloscope (Tektronix model TDS 210, 60 MHz). Filters were used to bring the signals from all the samples in the same range. Urea with particle size ~150 μm was used as the reference (1 U = SHG of urea). Calibration measurements were carried out using *N*-4-nitrophenyl-(*S*)-prolinol (NPP).

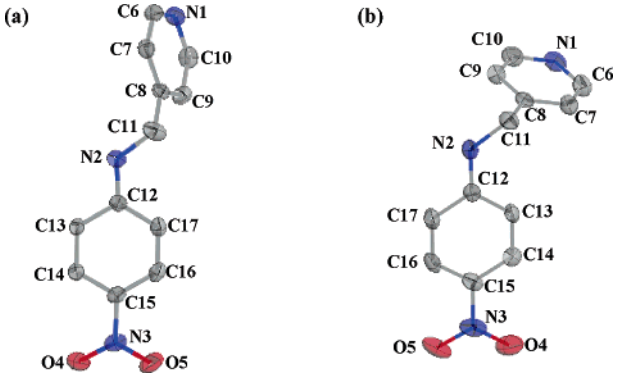

Figure 1. Molecular structure of PINA in (a) PINA-C and (b) PINA-N from single-crystal X-ray analysis. H atoms are omitted for clarity, and 90% probability thermal ellipsoids are indicated. C (gray), N (blue), and O (red) atoms are indicated.

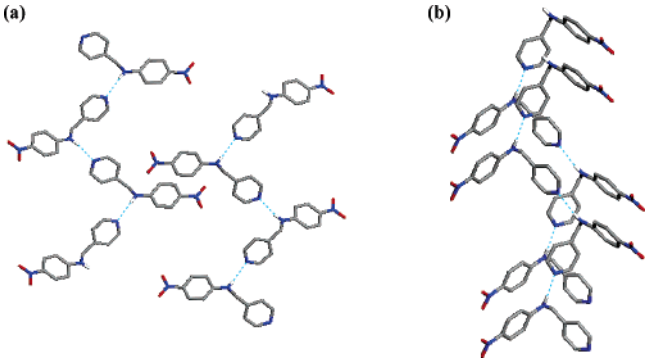

Figure 2. H-bonded chains of PINA formed along (a) the *a* axis in PINA-C and (b) the *c* axis in PINA-N. H atoms except those involved in H-bonding are omitted for clarity. C (gray), H (white), N (blue), and O (red) atoms and an H-bond (broken cyan line) are indicated.

Semiempirical Computations. Geometries of the molecules and molecular clusters for the computations were taken from the crystal structure, and hydrogen atoms alone were optimized using the semiempirical AM1 method[13] in the program suite MOPAC93.[14] Hyperpolarizabilities were computed using the TDHF method[15] available in MOPAC93; the values reported are the magnitude of β_{vec}, conventionally defined using the *x*, *y*, and *z* projections of the various tensorial components. β_0, the static value, as well as $\beta_{1.17}$ for excitation wavelength of 1064 nm are presented.

Results and Discussion

Two polymorphs of PINA could be crystallized depending on the solvent employed. Ethyl acetate−hexane yielded centrosymmetric crystals (PINA-C) belonging to the orthorhombic space group *Pbca*, whereas noncentrosymmetric crystals (PINA-N) belonging to the monoclinic space group *Pn* were obtained from acetonitrile−water solution. The crystallographic data for the two are collected in Table 1. The molecular structures in the two crystals are very similar (Figure 1) except for the link between the 4-picolyl group and pNA moiety; the dihedral angle C12−N2−C11−C8 is respectively 121.9 and 80.7° in PINA-C and PINA-N. In

(11) (a) *SAINT-Plus*, version 6.45; Bruker AXS: Madison, WI, 2003. (b) *SHELXTL*, version 6.14; Bruker AXS: Madison, WI, 2003.
(12) Kurtz, S. K.; Perry, T. T. *J. Appl. Phys.* **1968**, *39*, 3798.
(13) Dewar, M. J. S.; Zoebisch, E. G.; Healy, E. F.; Stewart, J. J. P. *J. Am. Chem. Soc.* **1985**, *107*, 3902.
(14) *MOPAC93*; Fujitsu, Inc.: Tokyo, 1993.
(15) Dupuis, M.; Karna, S. *J. Comput. Chem.* **1991**, *12*, 487.

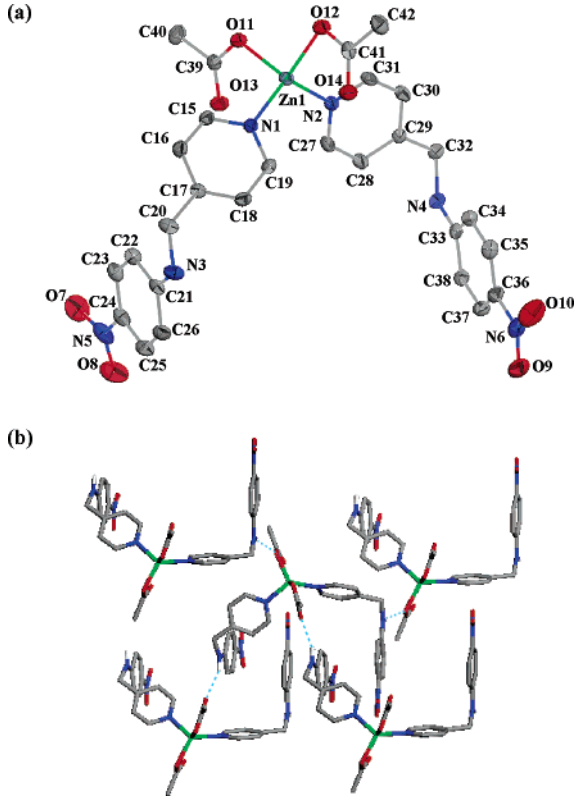

Figure 3. (a) Molecular structure of ZPA from single-crystal X-ray analysis. H atoms are omitted for clarity, and 75% probability thermal ellipsoids are indicated. (b) H-bonding around each molecule of ZPA. H atoms except those involved in H-bonding are omitted for clarity. C (gray), H (white), N (blue), O (red), and Zn (green) atoms and an H-bond (broken cyan line) are indicated.

Table 2. Significant Bond Lengths in ZPA and ZPP

cryst	bond	bond length (Å)
ZPA	Zn1−N1	2.042(2)
	Zn1−N2	2.038(2)
	Zn1−O11	1.962(2)
	Zn1−O12	2.040(2)
ZPP	Zn1−N1	2.050(2)
	Zn1−O6	1.9670(17)

both the crystals, the PINA molecules are assembled into extended chain structures through intermolecular H-bonds formed between the amino nitrogen and pyridine nitrogen atoms: $r_{N2\cdots N1} = 2.967$ Å, $\theta_{N2-H2\cdots N1} = 147.1°$ in PINA-C; $r_{N2\cdots N1} = 2.966$ Å, $\theta_{N2-H2\cdots N1} = 165.2°$ in PINA-N. Figure 2a shows the adjacent chains formed along the *a* axis, related by a center of inversion in PINA-C; the chains formed along the *c* axis in PINA-N are shown in Figure 2b.

Crystals of Zn(II) acetate complex, ZPA grown from methanol are found to belong to the monoclinic space group *Pn* with one molecule in the asymmetric unit (Figure 3a, Table 1). Zn(II) is tetrahedrally coordinated by the pyridine nitrogen of two PINA molecules and the oxygen of two acetate ions; the significant bond lengths are collected in Table 2. The pNA moieties in the PINA ligands are oriented away from the direction of the acetate ligands; the torsion angle between the bisector of the O11−Zn1−O12 angle and the dipole vector of the pNA moieties N3−N5 and N4−N6 is respectively 110.3 and 137.3°. Each ZPA molecule is engaged in four H-bonds around it (Figure 3b) involving the

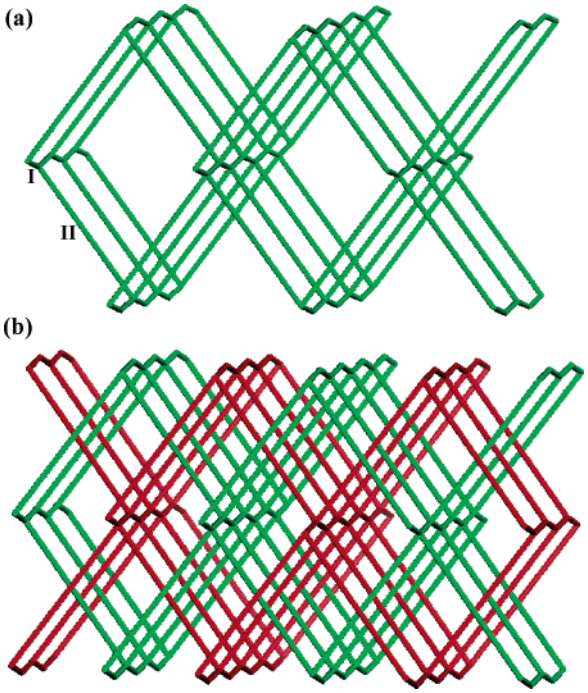

Figure 4. Schematic diagram of the (a) the extended net and (b) interpenetrating network (the two nets colored differently for clarity) formed through the H-bond assembly of ZPA molecules. The vertexes represent the Zn(II) ions and the edges the connectivity between corresponding molecules mediated by H-bonds: (I) $r_{Zn\cdots Zn} = 10.094$ Å (N8−H8···O12); (II) $r_{Zn\cdots Zn} = 12.188$ Å (N4−H4···O13).

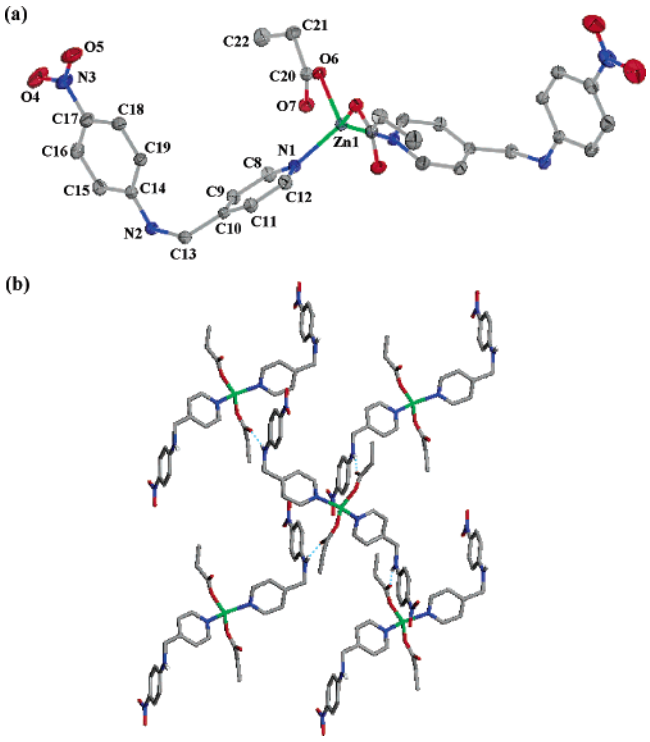

Figure 5. (a) Molecular structure of ZPP from single-crystal X-ray analysis. H-atoms are omitted for clarity, and 75% probability thermal ellipsoids are indicated. (b) H-bonding around each molecule of ZPP. H-atoms except those involved in H-bonding are omitted for clarity. C (gray), H (white), N (blue), O (red), and Zn (green) atoms and an H-bond (broken cyan line) are indicated.

amino and acetate groups; the independent ones correspond to $r_{N3\cdots O12} = 3.017$ Å, $\theta_{N3-H3\cdots O12} = 149.0°$ and $r_{N4\cdots O13} =$

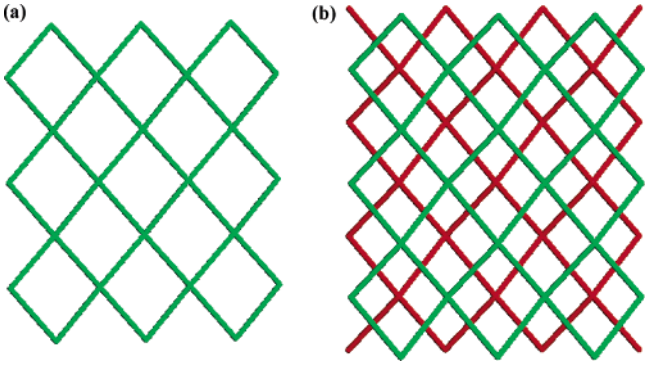

Figure 6. Schematic diagram of the (a) the extended net and (b) noninterpenetrating adjacent nets (the two nets colored differently for clarity) formed through the H-bond assembly of ZPP molecules. The vertexes represent the Zn(II) ions and the edges the connectivity between the corresponding molecules mediated by H-bonds: $r_{Zn\cdots Zn} = 11.911$ Å (N2−H2···O7).

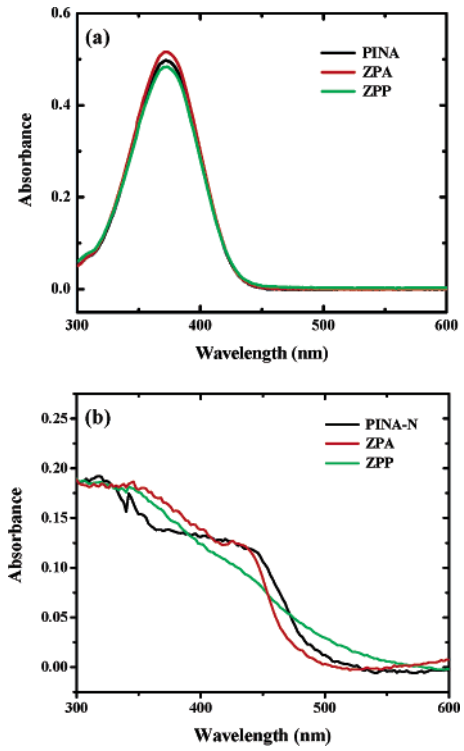

Figure 7. Electronic absorption spectra of PINA and its zinc(II) complexes in (a) solution state and (b) solid state.

2.901 Å, $\theta_{N4-H4\cdots O13} = 149.7°$. These H-bonds assemble ZPA molecules into a 3-dimensional interpenetrating network structure (Figure 4).

Crystals of ZPP grown from methanol belong to the orthorhombic space group $C222_1$ with half the molecule in the asymmetric unit (structure of the full molecule is shown in Figure 5a); crystallographic data are provided in Table 1. Coordination around Zn(II) is similar to that in the case of ZPA (the significant bond lengths are listed in Table 2); however, the pNA moieties in the ligands are now oriented in the direction of the propionate ligands so that the torsion angle between the bisector of the O6−Zn1−O6′ angle and the dipole vector of the pNA moieties, N2−N3, is 28.0°. Each ZPP molecule is engaged in four similar H-bonds (Figure 5b) involving the amino and propionate groups: $r_{N2\cdots O7} = 2.897$ Å, $\theta_{N2-H2\cdots O7} = 167.3°$. These H-bonds connect the molecules into a noninterpenetrating network structure (Figure 6) that extends parallel to the *bc* plane. Thus, the H-bonded assembly of ZPA and ZPP share some common features but exhibit significant differences as well.

Table 3. Powder SHG Data for PINA-N, ZPA, and ZPP (1 U = SHG of Urea with Particle Size > 150 μM)

	SHG (U)		
av particle size (μm)	PINA-N	ZPA	ZPP
40	2.09	5.36	0.21
75	2.85	6.53	0.22
125	2.97	11.63	0.23
175	3.14	12.43	0.24
225	3.35	14.81	0.25
275	3.38	15.05	0.28

Electronic absorption spectra of PINA as well as the zinc complexes are shown in Figure 7. The three compounds show nearly identical solution spectra with a peak at ∼370 nm. The absorption is much broader in the solid state, as expected from the impact of intermolecular interactions on the electronic structure; it falls off near 500 nm in all cases so that the materials are nearly transparent at the wavelength at which the SHG is measured in our study (532 nm). Results of the Kurtz−Perry powder SHG studies[12] on the different materials are collected in Table 3. The particle size dependence of the SHG indicates that all the compounds show phase-matchable behavior. The SHG observed in ZPA (∼15 U) is considerably enhanced with respect to that of PINA-N; however, on changing the counterion from acetate to propionate in ZPP, the SHG is reduced below that of PINA-N. Even though a judicious choice of metal ion can enhance the molecular hyperpolarizability,[16] metal complexation in many instances has the opposite impact and/or enforces nonoptimal orientation of the NLO-phores resulting in low SHG in the bulk material. Among the SHG active zinc complexes reported earlier, those showing strong response are rare;[10,17] the majority of them exhibit SHG well below 10.0 U[9,18] (see Supporting Information for a more extensive list of references). The relatively high value of ZPA is notable and indicates that the remote functionality approach has enabled an efficient exploitation of the NLO response of the molecular units. As described below, this approach also facilitates convenient analysis of the basis of the observed SHG response of the two zinc complexes. Even though the powder SHG is an average measure and does not provide

(16) (a) Roberto, D.; Ugo, R.; Bruni, S.; Cariati, E.; Cariati, F.; Fantucci, P.; Invernizzi, I.; Quici, S.; Ledoux, I.; Zyss, J. *Organometallics* **2000**, *19*, 1775. (b) Lacroix, P. G. *Eur. J. Inorg. Chem.*. **2001**, 339. (c) Roberto, D.; Ugo, R.; Tessore, F.; Lucenti, E.; Quici, S.; Vezza, S.; Fantucci, P.; Invernizzi, I.; Bruni, S.; Ledoux-Rak, I.; Zyss, J. *Organometallics* **2002**, *21*, 161. (d) Lacroix, P G.; Averseng, F.; Malfant, I.; Nakatani, K. *Inorg. Chim. Acta* **2004**, *357*, 3825. (e) Maury, O.; Viau, L.; Senechal, K.; Corre, B.; Guegan, J.; Renouard, T.; Ledoux, I.; Zyss, J.; Le Bozec, H. *Chem.—Eur. J.* **2004**, *10*, 4454. (f) Tancrez, N.; Feuvrie, C.; Ledoux, I.; Zyss, J.; Toupet, L.; Le Bozec, H.; Maury, O. *J. Am. Chem. Soc.* **2005**, *127*, 13474. (g) Tessore, F.; Roberto, D.; Ugo, R.; Pizzotti, M.; Quici, S.; Cavazzini, M.; Bruni, S.; De Angelis, F. *Inorg. Chem.* **2005**, *44*, 8967.

(17) (a) Lin, W.; Evans, O. R.; Xiong, R.; Wang, Z. *J. Am. Chem. Soc.* **1998**, *120*, 13272. (b) Evans, O. R.; Lin, W. *Chem. Mater.* **2001**, *13*, 3009. (c) Ye, Q.; Li, Y.; Song, Y.; Huang, X.; Xiong, R.; Xue, Z. *Inorg. Chem.* **2005**, *44*, 3618.

Table 4. AM1/TDHF Computed Hyperpolarizabilities (β_0 and $\beta_{1.17}$) of ZPA and ZPP Molecules, the Molecular Clusters in Their Unit Cells (Figure 8a,c), PINA Ligand Pair in ZPA and ZPP Molecules, and PINA Ligand Clusters in the Unit Cells (Figure 8b,d)[a]

	β_0 (10^{-30} esu)		$\beta_{1.17}$ (10^{-30} esu)	
system	ZPA	ZPP	ZPA	ZPP
molecule	8.222	9.035	16.337	17.711
molecular cluster in the unit cell	10.623 (5.312)	9.805 (2.451)	21.315 (10.658)	19.497 (4.874)
ligand pair in the molecule	8.425 (4.213)	11.648 (5.824)	17.364 (8.682)	22.273 (11.137)
ligand cluster in the unit cell	11.081 (2.770)	11.245 (1.406)	22.725 (5.681)	23.605 (2.951)

[a] The value *per molecule* in the case of molecular clusters or *per PINA unit* in the case of ligand clusters is indicated in parentheses.

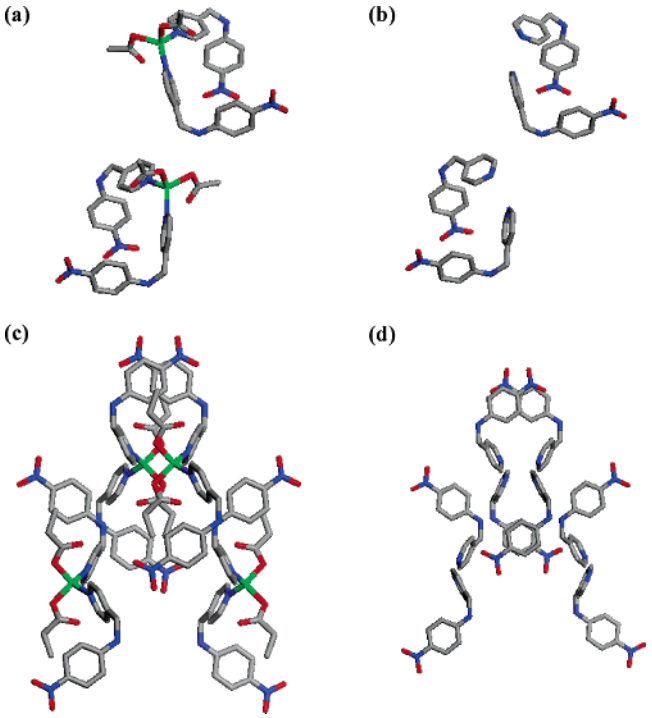

Figure 8. Molecular clusters considered in the computations: (a) unit cell of ZPA; (b) PINA in the unit cell of ZPA; (c) unit cell of ZPP; (d) PINA in the unit cell of ZPP. C (gray), N (blue), O (red), and Zn (green) atoms are indicated.

details of the nonlinear susceptibility tensor components, useful insight into the observed trends can be gained through semiempirical quantum chemical computations.

Computations were carried out on molecular structures determined from the single-crystal analysis. The hyperpolarizabilities computed for single molecules of ZPA and ZPP as well as the cluster of symmetry-related ones in the unit cell, two in ZPA and four in ZPP (Figure 8a,c), are collected in Table 4. The NLO response is dominated by the ligands since they bear the primary NLO-phore unit pNA; the contribution of the metal link attached to the remote functional units is likely to be small. This aspect was probed through computations on the pair of PINA ligands in ZPA and ZPP retaining their relative orientations, by excising out the zinc salt; the clusters of ligands in the unit cells (Figure 8b,d) were also considered in the study. Table 4 provides the computed values for these systems as well. The relative orientation of the pNA units leads to a slightly larger β in ZPP compared to ZPA; the torsion angle between the dipole vectors is 60.2 and 117.3° in ZPP and ZPA, respectively. It is seen that the NLO response of the PINA ligands is very close to that of the respective complexes, supporting the assumption of the remote nature of metal complexation. The slight decrease in the β of the ligands on complexation arises due to the oppositely directed nonlinear response of the pyridine−Zn(II) unit with respect to that of the pNA moiety. The most significant finding from the study is the following. Even though at the molecular level the nonlinear response of ZPP is stronger than that of ZPA, the response *per molecule* or *per PINA unit* at the crystal level is considerably weaker in ZPP. Examination of Figure 8 reveals that this stems from the orientation of the pNA units that tends to cancel out the response from each other to a large extent in ZPP whereas, in ZPA, they are conducive to producing appreciable SHG. The difference between ZPA and ZPP at the molecular level is the counterion. This leads to the different molecular conformations and extended H-bonded network structures in the two crystal lattices that together enforce the relative orientation of the NLO-phore units, determining the bulk SHG response. The computational exercise explains why the bulk SHG observed in ZPA is stronger than that in ZPP. It demonstrates also that the analysis of the bulk SHG in terms of the response of the NLO-phore units is facilitated by the remote functional nature of the ligand sites that ensured that the metal-mediated assembly did not influence the NLO-phore unit considerably. This provides a new direction for the systematic fabrication of quadratic NLO materials through the metal complexation route.

Conclusions

A simple ligand involving the classical NLO-phore, pNA, is designed with an appropriate remote functional group that enables the assembly through metal complexation. The free ligand is shown to form polymorphic structures, one of them being noncentrosymmetric and SHG active. Assembly of the ligand molecule through Zn(II) complexation and H-bonding leads to noncentrosymmetric and SHG active materials with the lattice structure sensitively dependent on the anion. The complex with zinc(II) acetate shows an interpenetrating 3-dimensional network structure formed through intermolecular H-bond interactions. The observed SHG of the metal complexes is rationalized using semiempirical computations

(18) (a) Qin, J.; Su, N.; Dai, C.; Yang, C.; Liu, D.; Day, M. W.; Wu, B.; Chen, C. *Polyhedron* **1999**, *18*, 3461. (b) Wang, X. Q.; Xu, D.; Yuan, D. R.; Tian, Y. P.; Yu, W. T.; Sun, S. Y.; Yang, Z. H.; Fang, Q.; Lu, M. K.; Yan, Y. X.; Meng, F. Q.; Guo, S. Y.; Zhang G. H.; Jiang M. H. *Mater. Res. Bull.* **1999**, 34, 2003. (c) Evans, C. C.; Masse, R.; Nicoud, J.; Bagieu-Beucher, M. *J. Mater. Chem.* **2000**, *10*, 1419. (d) Evans, O. R.; Lin, W. *Acc. Chem. Res.* **2002**, *35*, 511. (e) Han, L.; Hong, M.; Wang, R.; Luo, J.; Lin, Z.; Yuan, D. *Chem. Commun.* **2003**, 2580. (f) Ren, P.; Liu, T.; Qin, J.; Chen, C. *J. Coord. Chem.* **2003**, *56*, 125.

of the hyperpolarizabilities of molecules and supramolecular assemblies in the unit cell. This study suggests that noncentrosymmetric and SHG active crystal lattices of NLO-phores may be constructed through appropriate ligand design and metal complexation and that the structure and function are affected by subtle changes in the linking units. The remote functional approach allows convenient analysis of the bulk SHG in terms of the molecular responses, facilitating the design of novel quadratic NLO materials based on metal complexes.

Acknowledgment. Financial support from the CSIR and DST, New Delhi, and use of the National Single Crystal X-ray Diffractometer Facility at the School of Chemistry and the Universities with Potential for Excellence Program of the UGC, New Delhi, are acknowledged. M.J.P. thanks the CSIR, New Delhi, for a Senior Research Fellowship.

Supporting Information Available: Details of the crystal structure determination, crystallographic tables, powder X-ray patterns and simulations, a reference list, and computational details.

IC061145V